

Article

Carbon Nanotube Integration with a CMOS Process

Maximiliano S. Perez ¹, Betiana Lerner ^{1,*}, Daniel E. Resasco ², Pablo D. Pareja Obregon ³, Pedro M. Julian ³, Pablo S. Mandolesi ³, Fabian A. Buffa ⁴, Alfredo Boselli ¹ and Alberto Lamagna ¹

¹ Grupo MEMS, Comision Nacional de Energia Atomica, San Martin 1650, Buenos Aires, Argentina; E-Mails: mperez@cnea.gov.ar (M.S.P.); boselli@cnea.gov.ar (A.B.); alamagna@cnea.gov.ar (A.L.)

² School of Chemical, Biological and Materials Engineering, University of Oklahoma, Norman, OK 73019, USA; E-Mail: resasco@ou.edu

³ Departamento de Ingenieria Electrica y de Computadoras, Universidad Nacional del Sur, Bahia Blanca B8000FTN, Argentina; E-Mails: pablopereja@ieee.org (P.D.P.O.); pjulian@uns.edu.ar (P.M.J.); pmandolesi@uns.edu.ar (P.S.M.)

⁴ INTEMA Facultad de Ingenieria, Universidad Nacional de Mar del Plata, Mar del Plata B7608FDQ, Argentina; E-Mail: fbuffa@fi.mdp.edu.ar

* Author to whom correspondence should be addressed; E-Mail: blerner@cnea.gov.ar; Tel.: +54-11-6772-7931; Fax: +54-11-6772-7134.

Received: 27 January 2010; in revised form: 6 April 2010 / Accepted: 9 April 2010 /

Published: 15 April 2010

Abstract: This work shows the integration of a sensor based on carbon nanotubes using CMOS technology. A chip sensor (CS) was designed and manufactured using a 0.30 μm CMOS process, leaving a free window on the passivation layer that allowed the deposition of SWCNTs over the electrodes. We successfully investigated with the CS the effect of humidity and temperature on the electrical transport properties of SWCNTs. The possibility of a large scale integration of SWCNTs with CMOS process opens a new route in the design of more efficient, low cost sensors with high reproducibility in their manufacture.

Keywords: carbon nanotube sensor; CMOS integration; microchip sensor; SWCNT

Classification: PACS 85.35.-p, 85.35.Kt, 85.40.-e

1. Introduction

The development of carbon nanotube (CNT) sensors has been the subject of intense research in recent years. Due to their unique physical and electrical properties, CNT sensors have been shown to be good sensing elements for pressure [1], alcohol [2], gases [3,4] and biological molecules [5,6].

CNT sensors are mostly manufactured using basic lithography processes [7,8], in which reproducibility and resolution are limited to the manufacturing laboratory, making it difficult to scale up to volume manufacturing. Here we use complementary metal-oxide semiconductor (CMOS) technology to manufacture single wall carbon nanotube (SWCNT) sensors. This technology has been used for several years by the semiconductor industry, obtaining excellent reproducibility results in manufacturing. The CS are manufactured in batch technologies, where thousands of these can be generated from a single wafer, hence the cost of manufacturing is extremely reduced. In addition, this technology allows higher sensitivity through on chip signal processing.

To place the SWCNTs on the electrodes, a dielectrophoretic (DEP) process is used to improve the efficiency of SWCNT sensor fabrication. DEP is a phenomenon where neutral particles undergo mechanical motion inside an AC electric field [9,10]. The DEP force is a simple and effective methodology to assemble SWCNTs on electrodes and is compatible with commercial CMOS process [11].

As a result, these sensors are the union of sensing elements, interfacing and measurement circuitry in a single integrated chip with low power consumption, high reproducible manufacture and low cost, making possible the scale up of the sensors from the research laboratory prototype to a commercial product.

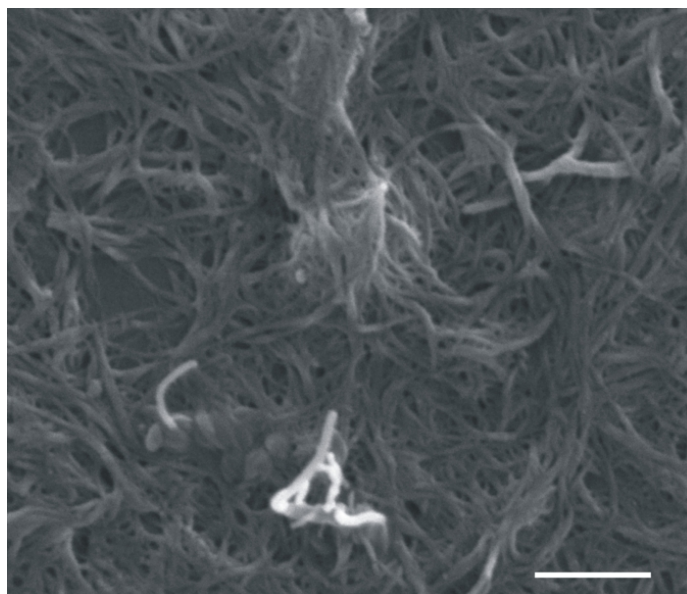
We investigated with the CS the effect of humidity and temperature on the electrical transport properties of SWCNTs. The experimentally transport properties of SWCNT network as a function of temperature are found consistent with a fluctuation induced tunneling mechanism due to the existence of contact barriers between individual nanotubes [12]. The energy barriers can exist as a result of contacts either between metallic and semiconductive nanotubes or between semiconductive nanotubes with different band gap.

2. Experimental Section

2.1. Carbon Nanotubes

The carbon nanotubes used in this study have been obtained by the catalytic CoMoCAT method [13], which employs a silica-supported Co-Mo powder to catalyze the selective growth of SWCNTs by disproportionation of CO. The SWCNTs grown by this method were purified by SWeNT (Southwest Nanotechnologies). The resulting nanotubes have an excellent quality [14] as determined by transmission electron microscopy (TEM), scanning electron microscopy (SEM) (Figure 1) and the D/G band ratio in the Raman spectra obtained at laser excitations of 633, 514, and 488 nm, as well as very low impurity content as determined by XPS analysis. The SWCNT used in this experiment have a semiconducting character [15,16] and have an average length of 300 nm.

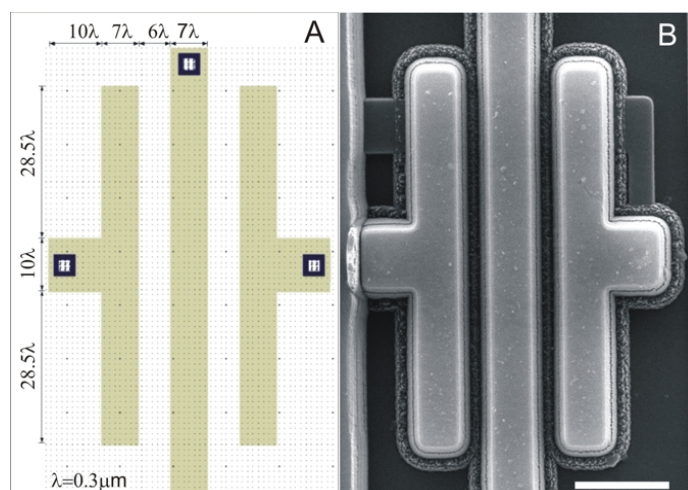
Figure 1. SEM micrograph of SWCNTs. Scale bar: 100 nm.



2.2. Chip Sensor

The top layer metal in the CMOS chip was designed to act as electrodes for the CS fabrication. Openings of the passivation layer were made to expose the electrodes in the CS design.

Figure 2. (A) Mask layout with electrode dimensions, (B) SEM micrograph of the electrodes. The gap between the electrodes is $1.3\ \mu\text{m}$. Scale bar: $10\ \mu\text{m}$.



The CS was fabricated using a commercial CMOS process; this achieves the required resolution with low cost and high reproducibility. The interface between the SWCNTs and the output signal was composed of a microelectronic circuit. This circuit takes the signals inherent to the measurement, and generates the amplification needed to obtain an output signal with low noise level. The amplification was made through a transresistance amplifier circuit. The integrated circuit was fabricated by MOSIS in the standard process AMIS 0.50 with a minimum size $\lambda = 0.3\ \mu\text{m}$. The design was made using Tanner L-Edit software. Figure 2 shows the dimensions of the electrodes.

2.3. Carbon Nanotube Deposition

We immersed the chip in 50% nitric acid solution for 12 s to remove the aluminum oxide layer formed on top of electrodes. Immediately after that, SWCNTs deposition was made over the chip. We used the DEP process to deposit the SWCNTs on the electrodes. An amount of 0.2 mg of SWCNTs were dispersed in 1 mL ethanol and ultrasonicated for 20 min with a high power horn sonicator. One microliter of this solution was put between the gap of the electrodes and an alternating voltage of 5 Vpp at a frequency of 1 MHz was applied to the opposite drain electrodes to generate the DEP force (Figure 3). After a few minutes, the ethanol was evaporated and the SWCNTs were aligned between the electrodes. Figure 4 shows the SWCNTs deposited between electrodes and Figure 5 shows stable I-V measurements before and after assemble SWCNTs, indicating that the DEP process worked correctly.

Figure 3. Scheme of the SWCNTs deposition by DEP process.

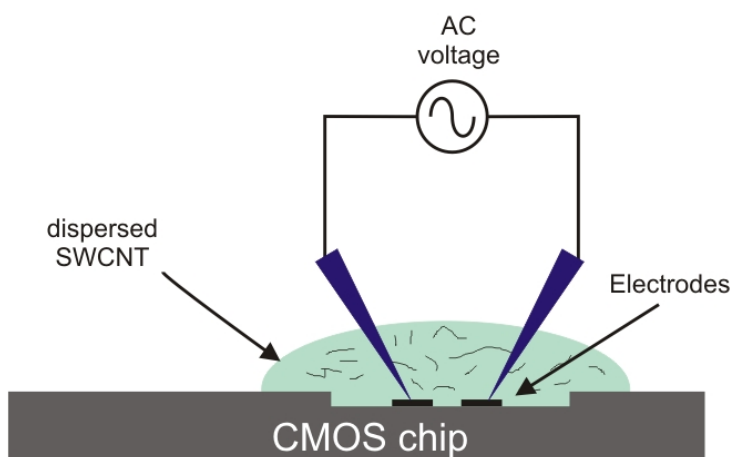


Figure 4. SEM micrograph of SWCNTs deposited between electrodes. Scale bar: 1 μm .

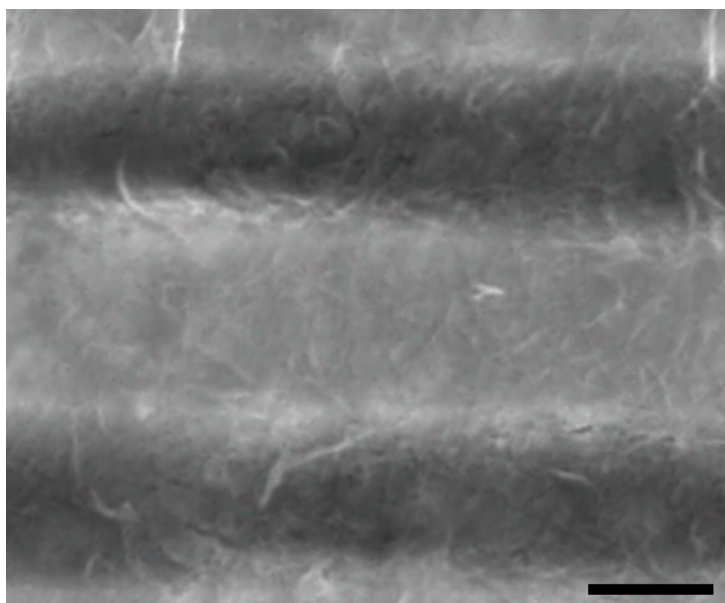
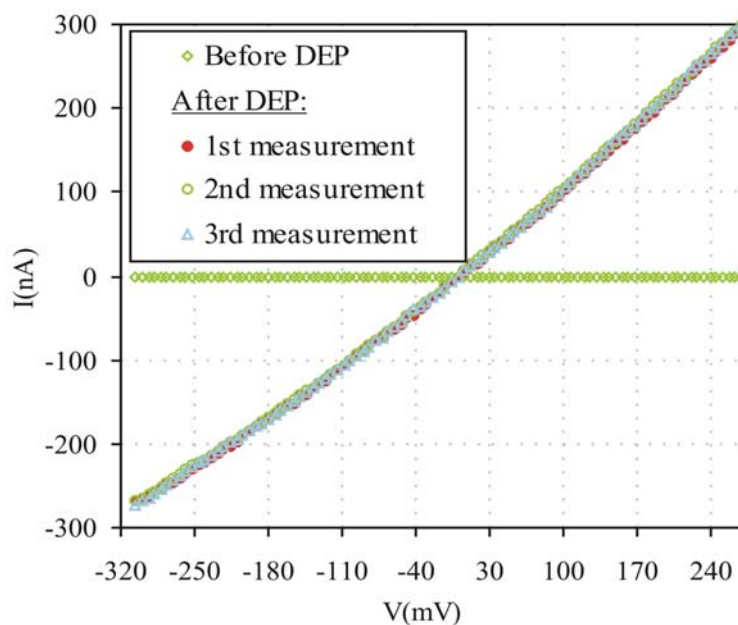


Figure 5. Current voltage characteristics of the SWCNTs assembled onto CMOS circuitry by DEP process.



2.4. Humidity Control and Electrical Measurements

CS were located in a chamber (volume 500 cc) where air flow at a constant rate of 300 sccm and humidity was controlled with a 0.1% precision at 298 K. Electrical measurements were taken immediately after the SWCNT deposition in order to avoid interference by aluminum oxide formation over the electrodes. Current was supplied by a Keithley 6221 current source and voltage changes were measured with a Keithley 2000 multimeter. Programming to manage data acquisition was performed in LABVIEW (National Instruments).

3. Results and Discussion

3.1. Chip Sensor Layout

We designed the CS with a free window on the passivation layer that allowed the deposition of SWCNTs over the electrodes. A scheme of the CS is shown in Figure 6. The CS has an arrangement of free electrodes formed by one common central source and several drains connected directly with the external pads and one arrangement of electrodes connected to an amplifier. The amplifier circuit comprises a current mirror, which reflects the input current of one of the pads on the SWCNTs to generate an output voltage (V_{out}) (Figure 7). This V_{out} is the input of an operational amplifier in a unity gain configuration, whose purpose is to act as a buffer and prevent the output voltage of the SWCNTs to be loaded or affected by any external circuit to the die.

Figure 6. Optical microscopy of the full chip. Inset shows the opening in the passivation layer with exposed electrodes. “A” indicates the electrodes connected to the amplifier. “B” indicates the free electrodes connected directly to the external pads.

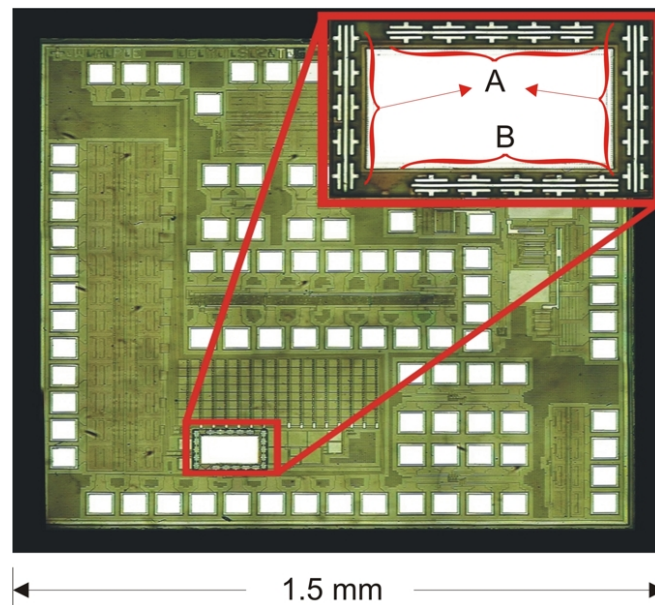
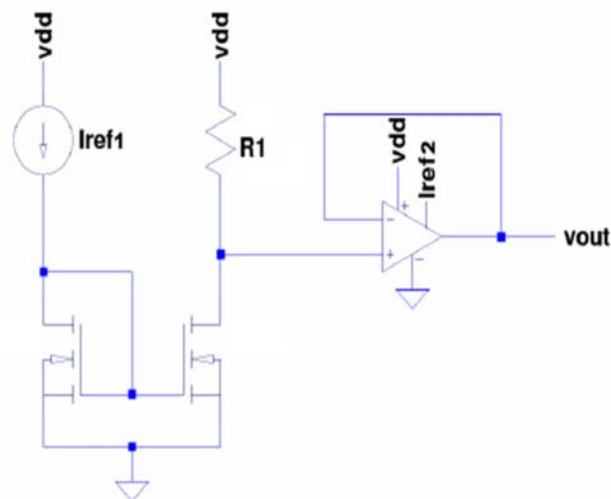


Figure 7. Schematic of the amplifier. Vdd: 5V, current reference 1 (Iref1): 2 μ A, current reference 2 (Iref2): 10 μ A, R1: SWCNT resistance; Vout: output voltage.



3.2. Effect of Humidity on the Electrical Transport Properties of SWCNTs

We examined the effect of the humidity changes on the resistance of SWCNTs. Figure 8 shows the effect of humidity over the current voltage characteristics of SWCNTs placed on the free electrodes. Under a modest humidity, the adsorbed water molecules appear to compensate the hole carriers in the SWCNTs, resulting in a increase in the resistance. When the humidity level becomes higher than 67%, the decreasing resistance is probably due to a surplus electron carrier. The possible influence of a contact resistance between electrodes and SWCNTs was recently addressed by other authors [17-19] and ruled out because the contact resistance present in two leads contacted samples provide a

comparatively low contact resistance relative to the resistance between the electrodes and the possible Schottky barriers formed at the SWCNTs-electrode interface have a negligible effect on the measurements.

We have also compared the effect of humidity on the SWCNTs placed on the electrodes connected to the amplifier with the ones placed on free electrodes. Figure 9 shows the simulated resistance of the SWCNTs made with Spice software from V_{out} values using Mosis parameters, compared with the SWCNTs resistance on the free electrodes. SWCNTs behavior as function of humidity changes was similar between electrodes connected to the amplifier and the free electrodes, and it is in agreement with what was previously reported by other authors [20,21], indicating that the CS works properly and the integration of CMOS process with SWCNTs was successful.

Figure 8. The effect of humidity over current voltage characteristics of SWCNTs detected through the free electrodes.

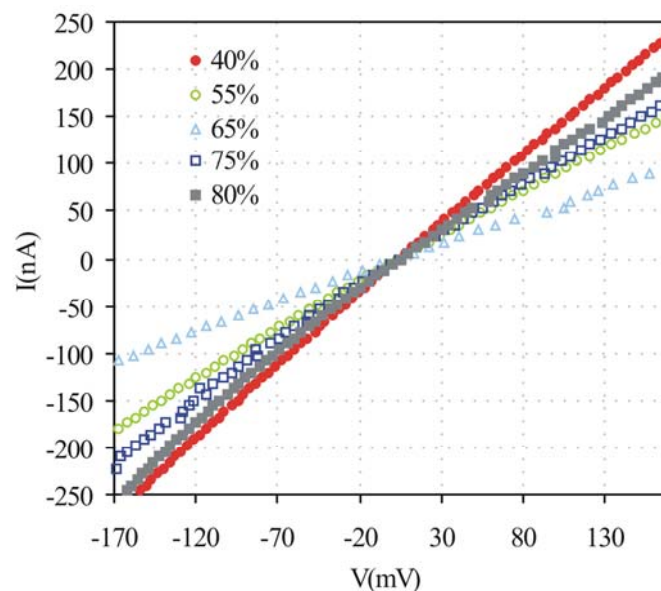
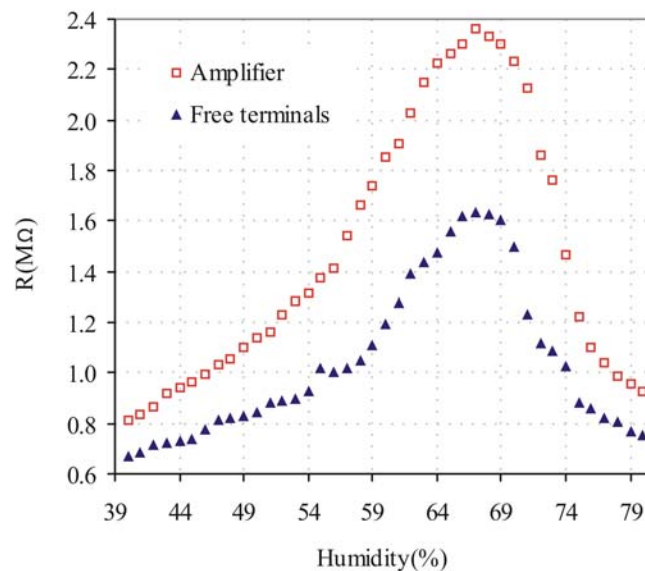


Figure 9. Effect of humidity over the resistance of SWCNTs detected by electrodes connected to the amplifier and free electrodes.



A difference (approx. 0.2–0.8 Mohm) between the resistance with the amplifier and the free electrodes was observed with a same humidity value. This difference can be attributed to a different amount of SWCNTs deposited between each electrode.

The resistance values taken by the electrodes connected to the amplifier showed more uniformity than those taken by the free electrodes, demonstrating that the electrodes connected to amplify have a better output signal with low noise level.

3.3. Effect of Temperature on the Electrical Transport Properties of SWCNTs

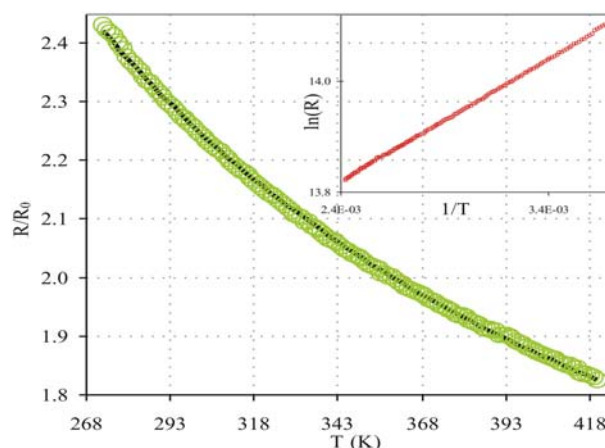
We studied the electrical transport characteristics of SWCNTs with the CS at different temperatures. Among the theoretical models that have been proposed to explain the observed experimental features in disordered heterogeneous systems [22,23] the Fluctuation Induced Tunneling (FIT) model [24] has been subject of attention [25]. The conduction electrons are delocalized here and free to move over very large distances as compared to atomic dimensions. In these systems electron transfer between large conductive segments separated by small insulating gaps dominates electrical conductivity.

The $R(T)$ dependence of SWCNT network was measured in the range of 273 to 420 K (Figure 10). In this temperature range, $R(T)$ dependence can be approximated by a FIT conductivity mechanism [12,24]:

$$R = R_0 e^{T_1/(T+T_0)} \quad (1)$$

In this expression R_0 is the resistance at room temperature, $T_1 = 2SV_0^2/(\pi k_B e^2 w)$ and $T_0 = 4\hbar SV_0^{3/2}/(\pi^2 w^2 k_B e^2 \sqrt{2m})$ with S and w being the junction surface and width respectively, V_0 is the depth of the potential well, m the electron mass, e the electron charge, and k_B and h ($\hbar = h/2\pi$) are the Boltzmann and Planck constants, respectively. The solid curve in Figure 10 fits to the data based on Equation (1). The fit is very good over the whole temperature range studied suggesting, in accordance with what was previously reported by other authors [19,26], that FIT mechanism can be used for these aligned SWCNTs on CS.

Figure 10. Resistance vs. temperature for SWCNTs deposited on electrodes connected to the amplifier. Line is fit to the data obtained from Equation (1) with fit parameters: $T_1 = 277$ K and $T_0 = 40$ K. The inset shows the data in a $\ln(R)$ vs. $1/T$ plot.



Here, it was shown that SWCNTs have a strong dependence of electrical resistance with temperature, which suggests their potential use of the CS as a thermistor.

4. Conclusions

In this work the feasibility of integration of a CMOS process with SWCNTs has been demonstrated. A dielectrophoresis assembly was used to deposit the SWCNTs over the electrodes. We successfully developed and tested at different humidities and temperatures a CS prototype which includes an amplifier and free electrodes. The SWCNT's resistance was shown to be sensitive to humidity changes within a specific range. Although the charge transfer effect from adsorbed H₂O molecules tends to saturate at a certain point, care for the humidity condition must be taken for SWCNT sensor applications. The charge carrier properties in SWCNTs between electrodes were studied at different temperatures. Experimental data was consistent with the fluctuations induced tunneling model that emphasizes the role of energy barriers between the nanotubes. CMOS technology has been used for several years in electronic devices. In this work we propose to develop a new application of this technology through which sensors with low power consumption, excellent precision and low cost can be obtained.

Acknowledgements

This work was supported by Comision Nacional de Energia Atomica (CNEA), Agencia Nacional de Promocion Cientifica y Tecnologica (projects PAE 2004, PAE 2006 Nodo Nanotec) and Consejo Nacional de Investigaciones Cientificas y Tecnicas (CONICET).

References and Notes

1. Fung, C.; Zhang, M.; Dong, Z.; Li, W. Fabrication of CNT-based MEMS piezoresistive pressure sensors using DEP nanoassembly. In *Proceedings of IEEE NANO 2005*, Nagoya, Japan, July 11–15, 2005; pp. 199–202.
2. Sin, M.L.Y.; Chow, G.C.T.; Wong, G.M.K.; Li, W.J.; Leong, P.H.W.; Wong, K.W. Ultralow-power alcohol vapor sensors using chemically functionalized multiwalled carbon nanotubes. *IEEE Trans. Nanotechnol.* **2007**, *6*, 571–577.
3. Kauffman, D.; Star, A. Carbon nanotube gas and vapor sensors. *Angew. Chem. Int. Ed.* **2008**, *47*, 6550–6571.
4. Terranova, M.; Lucci, M.; Orlanducci, S.; Tamburri, E.; Sessa, V.; Reale, A.; Di Carlo, A. Carbon nanotubes for gas detection: materials preparation and device assembly. *J. Phys-Condens. Mat.* **2007**, *19*, 225004.
5. Maehashi, K.; Katsura, T.; Kerman, K.; Takamura, Y.; Matsumoto, K.; Tamiya, E. Label-free protein biosensor based on aptamer-modified carbon nanotube field-effect transistors. *Anal. Chem.* **2007**, *79*, 782–787.

6. Chen, R.; Choi, H.; Bangsaruntip, S.; Yenilmez, E.; Tang, X.; Wang, Q.; Chang, Y.; Dai, H. An investigation of the mechanisms of electronic sensing of protein adsorption on carbon nanotube devices. *Nano Lett.* **2003**, *3*, 727.
7. Rodríguez, D.; Lerner, B.; Perez, M.S.; Ibañez, F.; Leyva, A.; Bonaparte, J.; Rinaldi, C.; Boselli, A.; Lamagna, A. In comparison of the gas sensing properties of thin film sno produced by rgt0 and pore wetting technique. In *Proceedings of the 13th International Symposium on Olfaction and Electronic Nose*, Brescia, Italy, April 2009; pp. 377–380.
8. Star, A.; Tu, E.; Niemann, J.; Gabriel, J.; Joiner, C.; Valcke, C. Label-free detection of DNA hybridization using carbon nanotube network field-effect transistors. *Proc. Natl. Acad. Sci. USA* **2006**, *103*, 921.
9. Pohl, H. *Dielectrophoresis: The Behavior of Neutral Matter in Nonuniform Electric Fields*; Cambridge University Press: Cambridge, UK, 1978.
10. Li, J.; Zhang, Q.; Yang, D.; Tian, J. Fabrication of carbon nanotube field effect transistors by AC dielectrophoresis method. *Carbon* **2004**, *42*, 2263–2267.
11. Chen, C.; Agarwal, V.; Sonkusale, S.; Dokmeci, M. The heterogeneous integration of single-walled carbon nanotubes onto complementary metal oxide semiconductor circuitry for sensing applications. *Nanotechnology* **2009**, *20*, 225302.
12. Kim, G.; Jhang, S.; Park, J.; Park, Y.; Roth, S. Non-ohmic current-voltage characteristics in single-wall carbon nanotube network. *Synth. Met.* **2001**, *117*, 123–126.
13. Resasco, D.; Alvarez, W.; Pompeo, F.; Balzano, L.; Herrera, J.; Kitiyanan, B.; Borgna, A. A scalable process for production of single-walled carbon nanotubes (SWNTs) by catalytic disproportionation of CO on a solid catalyst. *J. Nanopart. Res.* **2002**, *4*, 131–136.
14. Bachilo, S.; Balzano, L.; Herrera, J.; Pompeo, F.; Resasco, D.; Weisman, R. Narrow (n, m)-distribution of single-walled carbon nanotubes grown using a solid supported catalyst. *J. Am. Chem. Soc.* **2003**, *125*, 11186–11187.
15. Herrera, J.; Balzano, L.; Pompeo, F.; Resasco, D. Raman Characterization of single-walled nanotubes of various diameters obtained by catalytic disproportionation of CO. *J. Nanosci. Nanotechnol.* **2003**, *3*, 133–138.
16. Alvarez, W.; Pompeo, F.; Herrera, J.; Balzano, L.; Resasco, D. Characterization of single-walled carbon nanotubes (swnts) produced by co disproportionation on co- mo catalysts. *Chem. Mater.* **2002**, *14*, 1853–1858.
17. Pop, E.; Mann, D.; Cao, J.; Wang, Q.; Goodson, K.; Dai, H. Negative differential conductance and hot phonons in suspended nanotube molecular wires. *Phys. Rev. Lett.* **2005**, *95*, 155505.
18. Pop, E.; Mann, D.; Wang, Q.; Goodson, K.; Dai, H. Thermal conductance of an individual single-wall carbon nanotube above room temperature. *Nano Lett.* **2006**, *6*, 96–100.
19. Salvato, M.; Cirillo, M.; Lucci, M.; Orlanducci, S.; Ottaviani, I.; Terranova, M.; Toschi, F. Charge transport and tunneling in single-walled carbon nanotube bundles. *Phys. Rev. Lett.* **2008**, *101*, 246804.
20. Na, P.; Kim, H.; So, H.; Kong, K.; Chang, H.; Ryu, B.; Choi, Y.; Lee, J.; Kim, B.; Kim, J. Investigation of the humidity effect on the electrical properties of single-walled carbon nanotube transistors. *Appl. Phys. Lett.* **2005**, *87*, 093101.

21. Zahab, A.; Spina, L.; Poncharal, P.; Marliere, C. Water-vapor effect on the electrical conductivity of a single-walled carbon nanotube mat. *Phys. Rev. B* **2000**, *62*, 10000–10003.
22. Kaiser, A.; Düsberg, G.; Roth, S. Heterogeneous model for conduction in carbon nanotubes. *Phys. Rev. B* **1998**, *57*, 1418–1421.
23. Zhang, R.; Baxendale, M.; Peijs, T. Universal resistivity-strain dependence of carbon nanotube/polymer composites. *Phys. Rev. B* **2007**, *76*, 195433.
24. Sheng, P.; Sichel, E.; Gittleman, J. Fluctuation-induced tunneling conduction in carbon-polyvinylchloride composites. *Phys. Rev. Lett.* **1978**, *40*, 1197–1200.
25. Kaiser, A. Electronic transport properties of conducting polymers and carbon nanotubes. *Rep. Progr. Phys.* **2001**, *64*, 1–49.
26. Ksenevich, V.; Seliuta, D.; Martunas, Z.; Kasalynas, I.; Valusis, G.; Galibert, J.; Kozlov, M.; Samuilov, V. Charge carrier transport properties in single-walled carbon nanotube fibers. *Acta Phys. Pol. A Gen. Phys.* **2008**, *113*, 1039–1042.

© 2010 by the authors; licensee Molecular Diversity Preservation International, Basel, Switzerland. This article is an open-access article distributed under the terms and conditions of the Creative Commons Attribution license (<http://creativecommons.org/licenses/by/3.0/>).